Exploring nuclear shapes with the shell model: new perspectives

Javier Menéndez

University of Barcelona
Institute of Cosmos Sciences

Heavy Ion Laboratory, University of Warsaw

Warszawa, 29th May 2025

UNIVERSITAT DE BARCELONA
MINISTERIO DE CIENCIA, INNOVACIÓN Y UNIVERSIDADES
Financiado por la Unión Europea NextGenerationEU
AGENCIA ESTATAL DE INVESTIGACIÓN
ICCUB

Collaborators

D. Frycz, A. M. Romero, A. Rios

A. Poves

T. R. Rodríguez

B. Bally

Outline

Shapes and nuclei (a theorist's view)

Case study: ^{28}Si

Impact of deformation: $\beta\beta$ decay

Summary

Nuclear landscape

The goal of nuclear physics is a unified description of nuclear structure, across the nuclear chart and based on nuclear forces

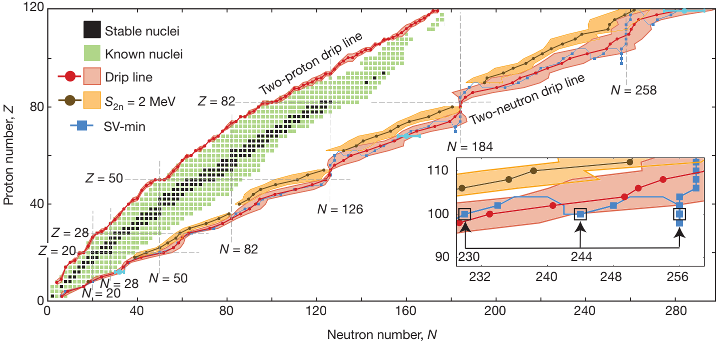

∼ 3000 isotopes measured

∼ 7000 predicted

Erler et al.
Nature 486 509 (2012)

Limits of existence, ground-state properties, shell evolution, excitation spectra, spectroscopy, shape coexistence, β decays, fission...

Outline

Shapes and nuclei (a theorist's view)

Case study: ^{28}Si

Impact of deformation: $\beta\beta$ decay

Summary

Spherical, deformed, superdeformed states

Deformation in nuclei: spherical, oblate, prolate, superdeformed

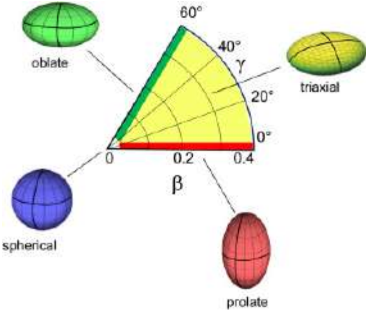

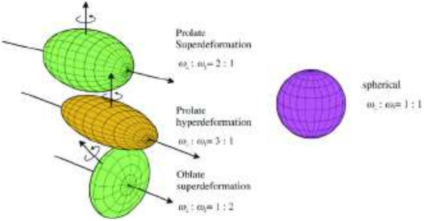

Leoni, Fornal, Bracco, Tsunoda, Otsuka, Prog. Part. Nucl. Phys. 139 104119 (2024)
Obertelli, Sagawa, Modern Nuclear Physics (2021)

Deformation parameters

$$\beta = \frac{4\pi}{3R_0^2 A}\frac{e_{\text{mass}}}{e}\sqrt{\langle\overline{Q}_{20}\rangle^2 + 2\langle\overline{Q}_{22}\rangle^2}, \qquad \gamma = \arctan\left(\frac{\sqrt{2}\langle\overline{Q}_{22}\rangle}{\langle\overline{Q}_{20}\rangle}\right)$$

Rotational bands in light nuclei

Rotational bands in light $N = Z$ nuclei identified early on
Shape coexistence with spherical ground state

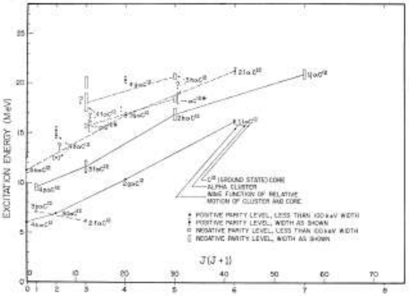

Carter et al. Phys. Rev. 133 B1421 (1964)

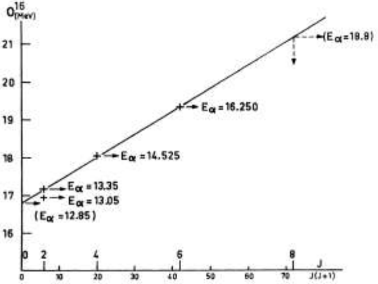

P. Chevallier et al. Phys. Rev. 160 827 (1967)

Energy spectrum: $E_J \propto J(J+1)$

Strong electric transitions: $B(E2; J_i \to J_f) = \frac{1}{2J_i+1} \left(J_f || Q_{20} || J_i\right)^2$

^{40}Ca: spherical, deformed, superdeformed bands

The Shell Model is the method of choice for medium-mass nuclei: energies, deformation, electromagnetic and β transition rates...

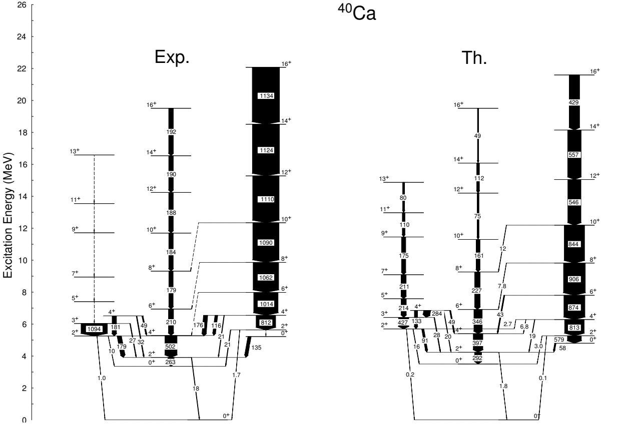

Ideguchi et al. PRL87 222501(2001)   Caurier, JM, Nowacki, Poves, PRC75 054317(2007)

^{42}Ca: spherical, superdeformed bands

Variational mean-field calculations also provide very useful insights

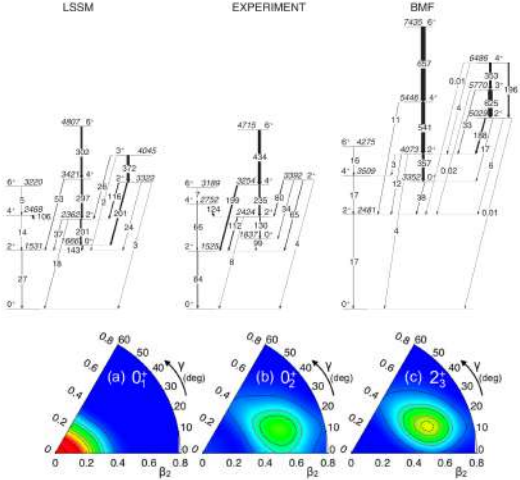

Hadynska-Klek et al. PRL117 062501(2016), PRC97 024326 (2018)

Shell model: insights from variational approach

In addition to comparison with observables valuable insights from description of nuclei in intrinsic frame

Results from variational solutions (eg mean field based) to shell-model Hamiltonian

Otsuka, Tsunoda, J.Phys.G 43, 024009 (2016)

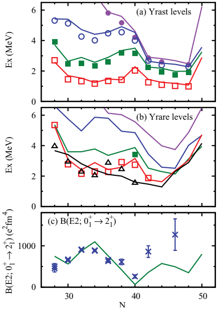

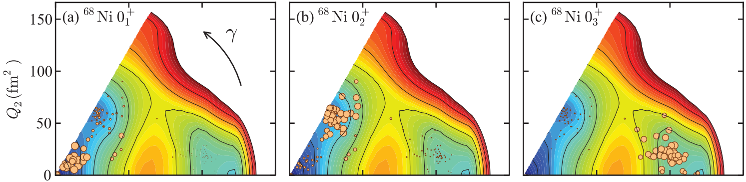

^{40}Ca: shape invariants

Need reference-frame independent (scalar!) quantities
to properly describe deformation: shape invariants

Kumar, Phys. Rev. Lett. 28, 249 (1972)
Cline, Ann. Rev. Part. Nucl. Sci. 36, 683 (1986)
Poves, Nowacki, Alhassid, Phys. Rev. C 101, 054307 (2020)

Couple quadrupole operator
to form scalars:

$$\langle [Q_2 \times Q_2]^0 \rangle \propto \beta^2$$

$$\langle [[Q_2 \times Q_2]^2 \times Q_2]^0 \rangle \propto \beta^3 \cos(3\gamma)$$

with uncertainties

$$\frac{\Delta\beta}{\beta} = \frac{\sqrt{\langle Q^4 \rangle - \langle Q^2 \rangle^2}}{2\langle Q^2 \rangle}$$

$$\frac{\Delta\gamma}{\gamma} = \ldots$$

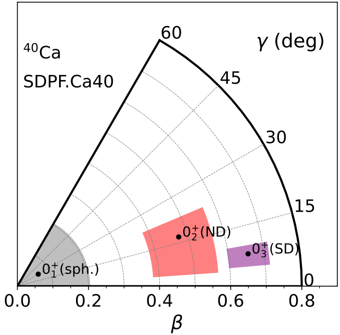

Frycz, Poves, JM, in preparation

^{40}Ca: shape invariants for bands

Need reference-frame independent (scalar!) quantities to properly describe deformation: shape invariants

Kumar, Phys. Rev. Lett. 28, 249 (1972)
Cline, Ann. Rev. Part. Nucl. Sci. 36, 683 (1986)
Poves, Nowacki, Alhassid, Phys. Rev. C 101, 054307 (2020)

Couple quadrupole operator to form scalars:

$$\langle [Q_2 \times Q_2]^0 \rangle \propto \beta^2$$

$$\langle [[Q_2 \times Q_2]^2 \times Q_2]^0 \rangle \propto \beta^3 \cos(3\gamma)$$

with uncertainties

$$\frac{\Delta\beta}{\beta} = \frac{\sqrt{\langle Q^4 \rangle - \langle Q^2 \rangle^2}}{2\langle Q^2 \rangle}$$

$$\frac{\Delta\gamma}{\gamma} = \ldots$$

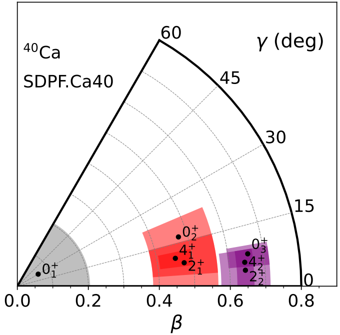

Frycz, Poves, JM, in preparation

Outline

Shapes and nuclei (a theorist's view)

Case study: ^{28}Si

Impact of deformation: $\beta\beta$ decay

Summary

^{28}Si: non-interacting shell model

In original shell-model picture, ^{28}Si would be a spherical nucleus

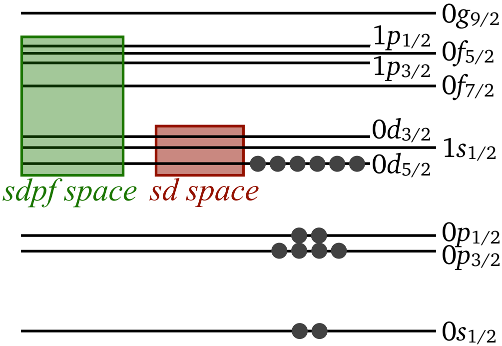

Frycz et al. 110 054326 (2024)

^{28}Si: shape coexistence

Experimentally, ^{28}Si shows coexistence of two different shapes:

- Ground-state oblate band
- Prolate band with bandhead at $\sim$ 6.5 MeV

Additionally, superdeformed band at $\sim$ 13 MeV suggested by antisymmetrized molecular dynamics

Taniguchi et al. PRC 80 044316 (2009)

But so far not found experimentally

Morris et al. PRC 104 054323 (2021)

Previous works do not describe well coexistence of oblate and prolate bands

Soyeur et al., Wildenthal et al., Vargas et al., Richter et al., Hinohara et al., Smirnova et al...

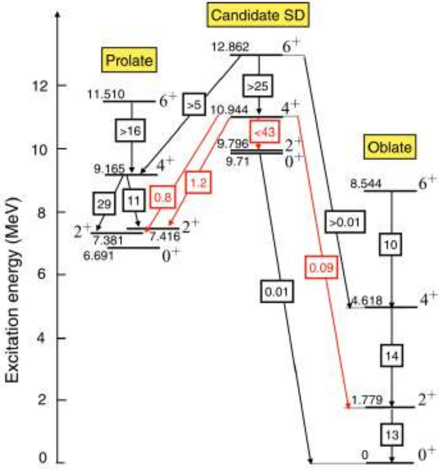

^{28}Si: interacting nuclear shell model

In modern shell-model calculations
^{28}Si includes, in general, a mixture of configurations

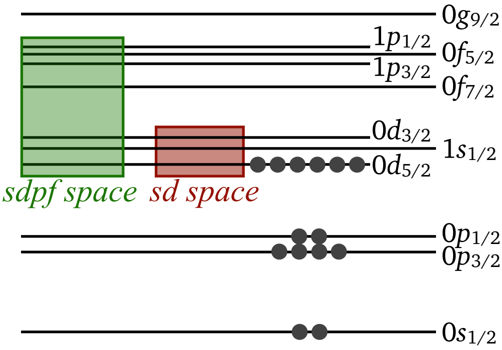

Frycz et al. 110 054326 (2024)

Nuclear shell model

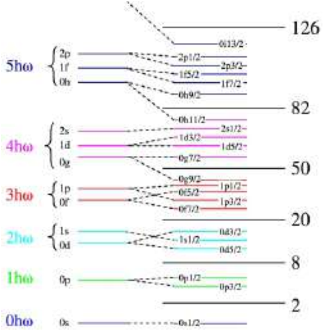

Only keep essential degrees of freedom

- High-energy orbitals: always empty
- Valence space:
  where many-body problem is solved
- Inert core: always filled

$$H\,|\Psi\rangle = E\,|\Psi\rangle \;\rightarrow\; H_{eff}\,|\Psi\rangle_{eff} = E\,|\Psi\rangle_{eff}$$

$$|\Psi\rangle_{eff} = \sum_{\alpha} c_{\alpha}\,|\phi_{\alpha}\rangle\,, \quad |\phi_{\alpha}\rangle = a^{+}_{i1} a^{+}_{i2} ... a^{+}_{iA}\,|0\rangle$$

Shell model diagonalization:

$\sim 10^{12}$ Slater dets. Caurier et al. RMP77 (2005)

$\gtrsim 10^{30}$ Slater dets. variational

Otsuka, Shimizu, Tsunoda: PScr. 92 063001 (2017)
Dao, Nowacki: PRC 105, 054314 (2022)
Bally, Rodríguez: EPJA 60 62 (2024)

H_{eff} includes effects of

- inert core
- high-energy orbitals

Shell-model scaling

Even for medium-mass nuclei
shell-model calculations become demanding toward the mid-shell

with number of Slater determinants (many-body basis states) reaching $\sim 10^{10}$ for relatively simple nuclei

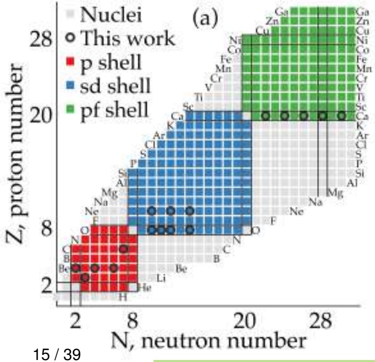

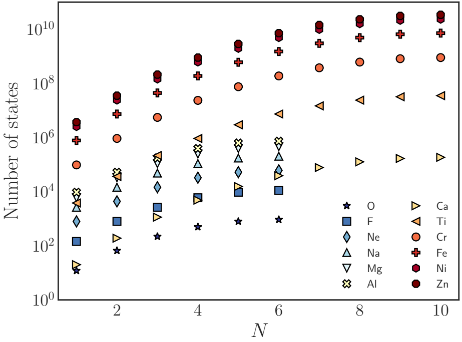

Nuclear shell model: computational power

Computational power critical for
size of nuclear shell model configuration space to be considered

1 major oscillator shell
$\sim 10^9$ Slater dets.
Caurier et al. RMP77 (2005)

$>$ 1 major oscillator shells
$\sim 10^{11}$ Slater dets.
Caurier et al. RMP77 (2005)

$\gtrsim 10^{24}$ Slater dets. variational
Otsuka, Shimizu, Tsunoda, Dao, Nowacki, Bally, Rodríguez

Nuclear shell model: variational method

Complement with multi-reference (variation after projection, conf. mixing)
variational method that pictures deformation of intrinsic state
same shell-model Hamiltonian and configuration space

Hartree-Fock-Bogoliubov basis states:

$$\beta_k^\dagger = \sum_l (U_{lk} c_l^\dagger + V_{lk} c_l)$$

constrained to β and γ values:

$$\mathcal{H}'_{\rm eff} = \mathcal{H}_{\rm eff} - \lambda_Z O_Z - \lambda_N O_N - \sum_i \lambda_i O_i \,,$$

projected to good quantum numbers:

$$|\phi^{NZJ}\rangle = P^N P^Z P^J_{MK} |\phi\rangle \,,$$

mixing via generalized coordinate method:

$$|\Psi^{NZJM}_{\sigma,{\rm GCM}}\rangle = \sum_{qK} f^{NZJM}_{\sigma;qK} |\phi^{NZJ}(q)\rangle \,,$$

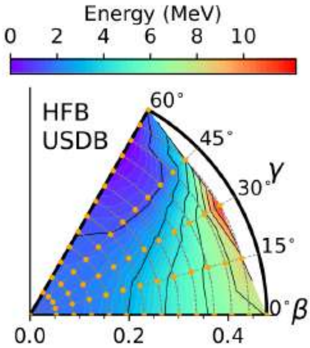

Taurus suite:
Bally et al. EPJA60 62 (2024)

UNIVERSITAT DE BARCELONA

Calculation of shape invariants

Calculation of shape invariants involve sum over all eigenstates connected by the Quadrupole operator

Kumar, Phys. Rev. Lett. 28, 249 (1972)

Cline, Ann. Rev. Part. Nucl. Sci. 36, 683 (1986)

Simpler calculation: only compute "Sum Rule" state (not eigenstate) exhausting the strength of Quadupole operator: $|SR\rangle = Q_2|I\rangle$

Poves, Nowacki, Alhassid Phys. Rev. C 101, 054307 (2020)

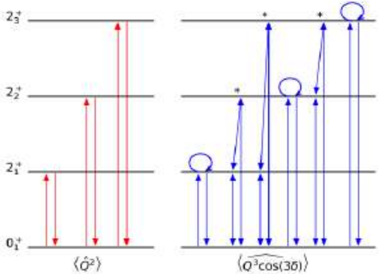

Henderson, PRC102, 054306 (2020)

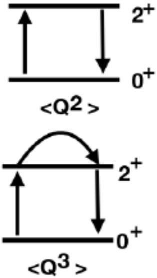

^{28}Si: shell-model vs experiment

Compare shell-model calculation with USDB interaction with experiment

Very good description of energies, B(E2) transitions ground-state oblate band (and associated vibration)

Poor description of B(E2) transitions of prolate band: not enough collectivity

In all cases
variational calculation
in very good agreement with diagonalization

Standard effective charges:
$e_n = 0.41e$, $e_p = 1.31e$

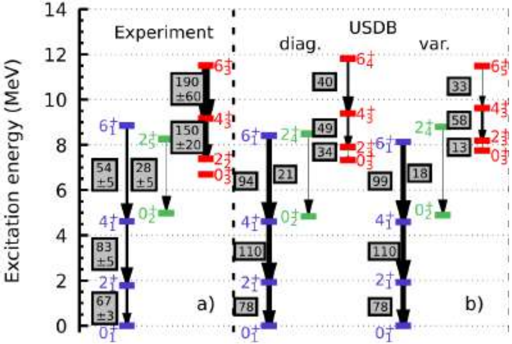

Frycz et al. PRC 110 054326 (2024)

^{28}Si: Shape invariants

Shape invariants confirm vibration character of the 0_2^+ state
coexistence of oblate and prolate deformations

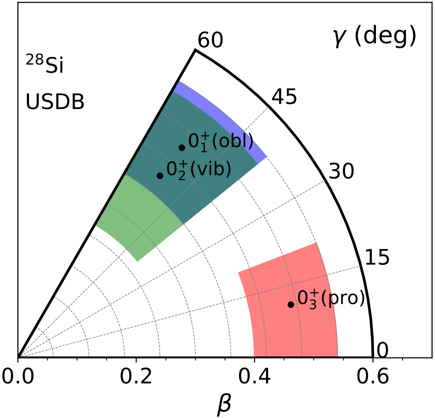

Frycz, Poves, JM, in preparation

Collective wavefunctions: oblate band

Collective wavefunctions obtained with variational method confirm well-defined oblate structure of ground-state band

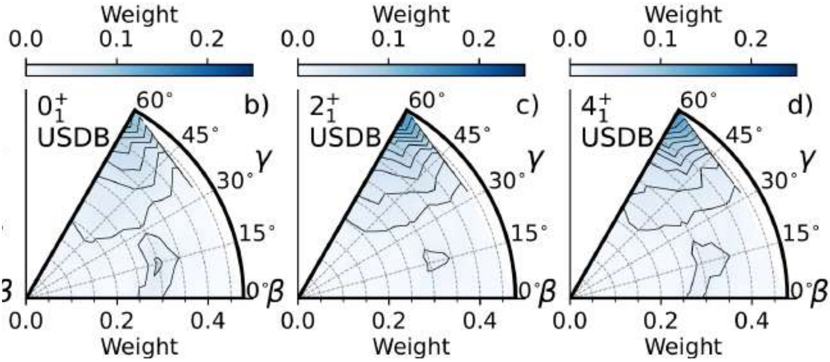

Frycz et al. PRC 110 054326 (2024)

Collective wavefunctions: vibration band

Vibration band based on ^{28}Si ground state at $\sim$ 5 MeV
shows consistent oblate collective wavefunctions

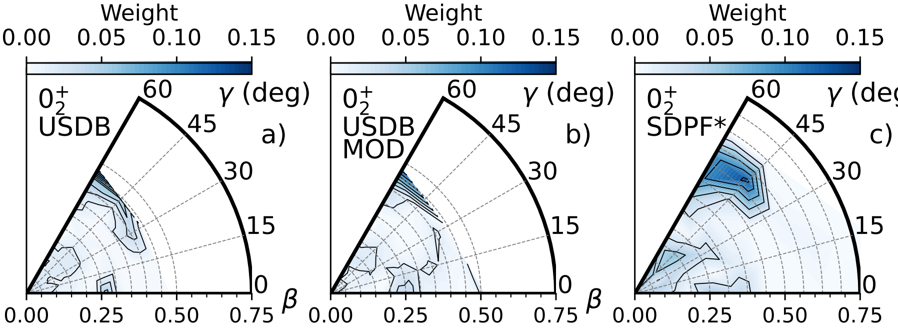

Frycz et al. PRC 110 054326 (2024)

Collective wavefunctions: prolate band

Collective wavefunctions obtained with variational method
confirm lack of well-defined structure for experimental prolate band
especially 0^+ state different to 2^+, 4^+ states

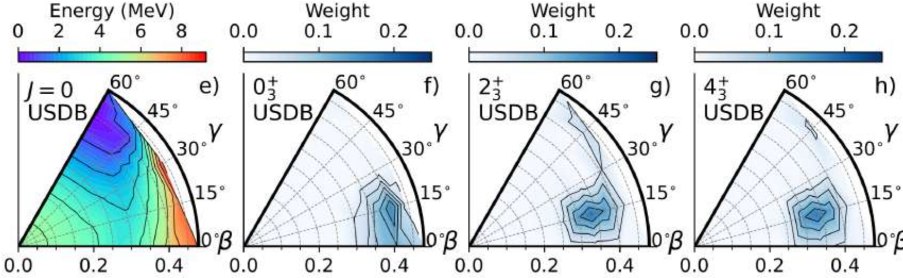

Frycz et al. PRC 110 054326 (2024)

How can prolate band be described by the nuclear shell model?

Deformation in shell model: SU(3) symmetry

Framework for deformation in shell model: Elliott's SU(3) symmetry

Elliott, Proc. R. Soc. Lon. Ser-A 245, 128 (1958)

Harmonic oscillator Hamiltonian with Quadrupole-Quadrupole interaction:

$$\mathcal{H} = \mathcal{H}_0 - \chi(Q_2 \cdot Q_2)$$

$E_J \propto J(J+1)$

Strong B(E2)'s within same SU(3) irrep

Quad. moment: $Q_0 = \sum_i (e_i\, Q_{0,i} \pm 3\tilde{e}) b^2$

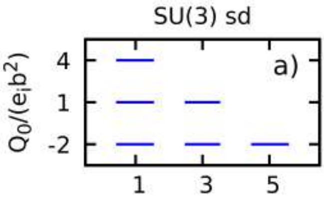

More realistic, with spin-orbit splitting: quasi-SU(3) symmetry

Zuker et al. Phys. Rev. C 52, R1741 (1995)

$\Delta l = 2$, $\Delta j = 2$ orbital pairs:
$d_{5/2} - s_{1/2}$ in sd shell

Treat $d_{3/2}$ orbital separately

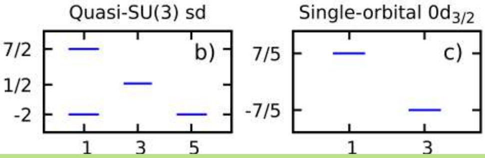

Quasi-SU(3) $0d_{5/2} - 1s_{1/2}$ prediction

Quasi-SU(3) model: oblate deformation with $0d_{5/2} - 1s_{1/2}$ structure

Prolate deformation with 4 nucleons excited into $0d_{5/2}$ orbital

	Q_0 (e fm^2)	
	Oblate	Prolate
Experiment	**-57.3 ± 0.7**	**72 ± 7**
Quasi-SU(3): $0d_{5/2} - 1s_{1/2}$+$0d_{3/2}$		
0p-0h	**-51.4**	33.3
2p-2h	−62.9	53.9
4p-4h	−74.4	**74.4**
6p-6h	−53.9	62.9
8p-8h	−33.3	51.4
SU(3): *sd*	−81.7	81.7

Deficiency of USDB interaction to describe prolate band associated with lack of excitations into $0d_{3/2}$ orbital

Propose USDB-MOD interaction, lower $0d_{3/2}$ energy by 1.2 MeV

Frycz et al. PRC 110 054326 (2024)

Prolate band beyond sd shell

However, USDB interaction “almost perfect” in sd shell:
USDB deficiency signature of necessity to go beyond sd shell?
Low-lying negative-parity states in ^{28}Si, spectroscopic factors...

Nann, NPA 376 61 (1982)

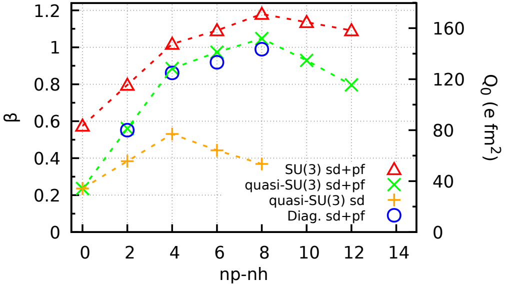

Frycz et al. PRC 110 054326 (2024)

Quasi-SU(3) analysis in sdpf configuration space

2p-2h excitations into the pf shell $\sim$ 4p-4h excitations into $d_{3/2}$ orbital

^{28}Si: sdpf calculation vs experiment

SDPF-NR* interaction, used for neutron-rich Si isotopes

S. Nummela et al. Phys. Rev. C 63, 044316 (2001)

monopole-adjusted to reproduce the sd-pf gap in ^{28}Si

Frycz et al. PRC 110 054326 (2024)

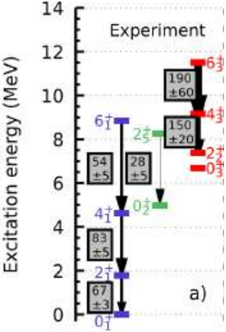

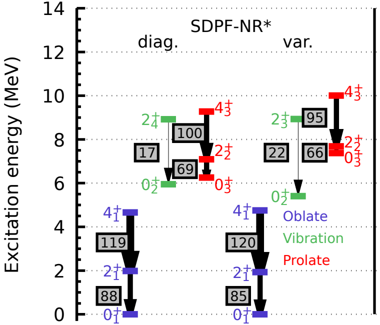

Good description of both oblate and prolate bands simultaneously!

25% of the prolate bandhead has 2p-2h sd-pf shell character

Collective wavefunctions for SDPF-NR*

Collective wavefunctions confirm well-defined oblate and prolate bands

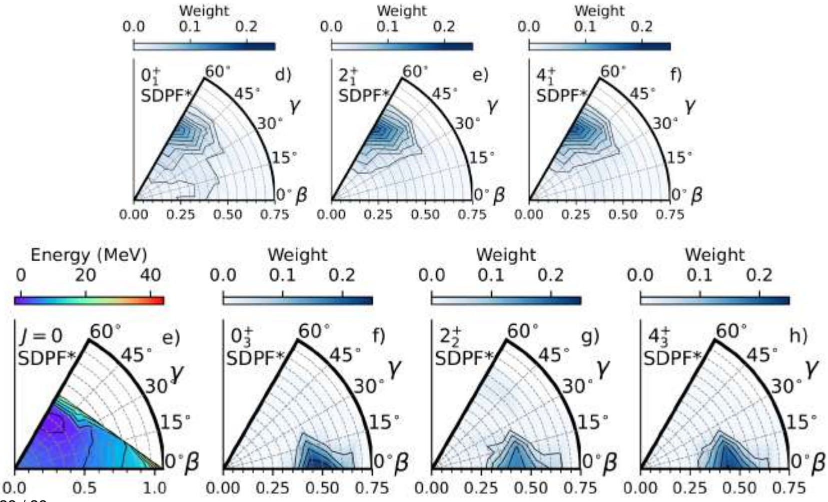

Superdeformed band in ^{28}Si?

Antisymmetrized molecular dynamics predicts
superdeformed prolate bandhead
cluster torus-like deformation
at $E \sim 13$ MeV

Taniguchi et al. PRC 80 044316 (2009)

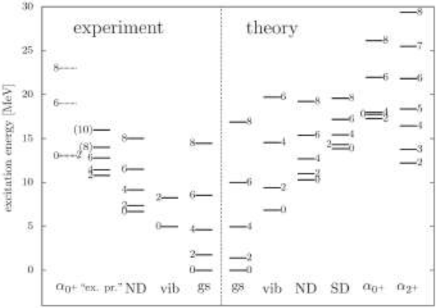

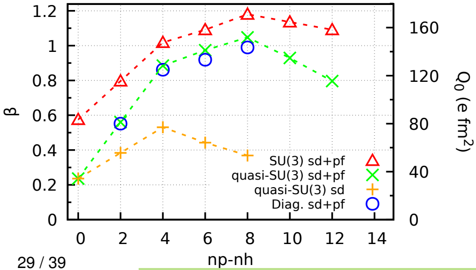

Quasi-SU(3) analysis:
superdeformed band needs
4p-4h excitations to pf shell

Frycz et al. PRC 110 054326 (2024)

Prediction for superdeformed band in ^{28}Si

Diagonalization and variational methods consistently suggest superdeformed states at energies $E \sim 18 - 20$ MeV
~ 6 MeV higher in energy than antisymmetrized molecular dynamics

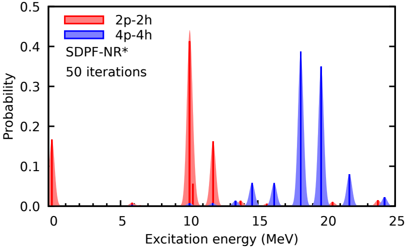

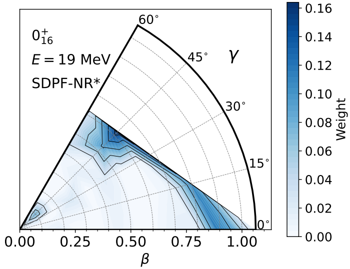

Lanczos strength function analysis of superdeformed 4p-4h structure fragmentation into two states at $E = 18$ MeV and $E = 20$ MeV

Variational analysis confirms superdeformed collective wavefunctions at $E \sim 19$ MeV (high-lying excited state) Frycz et al. PRC 110 054326 (2024)

Outline

Shapes and nuclei (a theorist's view)

Case study: ^{28}Si

Impact of deformation: $\beta\beta$ decay

Summary

Creation of matter in nuclei: $0\nu\beta\beta$ decay

Lepton number conserved in all processes observed:

single β decay,
$\beta\beta$ decay with ν emission...

Neutral massive particles (Majorana ν's) allow lepton number violation:

neutrinoless $\beta\beta$ decay
creates two matter particles (electrons)

Agostini, Benato, Detwiler, JM, Vissani, Rev. Mod. Phys. 95, 025002 (2023)

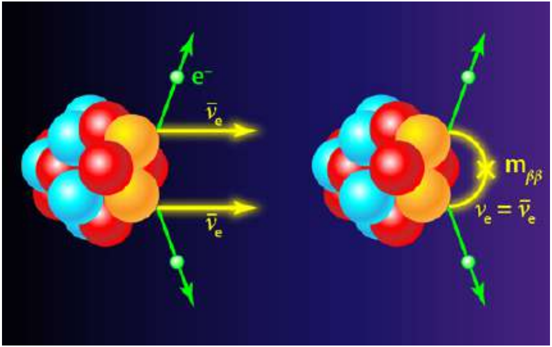

UNIVERSITAT DE BARCELONA

$\beta\beta$ decay

Second order process in the weak interaction

Only observable in nuclei where (much faster) β-decay is forbidden energetically due to nuclear pairing interaction

$$BE(A) = -a_v A + a_s A^{2/3} + a_c \frac{Z(Z-1)}{A^{1/3}} + \frac{(A-2Z)^2}{A} + \begin{cases} -\delta_{pairing} & \text{N,Z even} \\ 0 & \text{A odd} \\ \delta_{pairing} & \text{N,Z odd} \end{cases}$$

or where β-decay is very suppressed by ΔJ angular momentum change

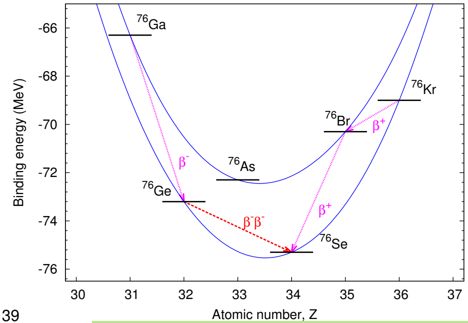

$^{48}Ca \to {}^{48}Ti$
$^{76}Ge \to {}^{76}Se$
$^{82}Se \to {}^{82}Kr$
$^{96}Zr \to {}^{96}Mo$
$^{100}Mo \to {}^{100}Ru$
$^{110}Pd \to {}^{110}Cd$
$^{116}Cd \to {}^{116}Sn$
$^{124}Sn \to {}^{124}Te$
$^{130}Te \to {}^{130}Xe$
$^{136}Xe \to {}^{136}Ba$
$^{150}Nd \to {}^{150}Sm$

Next generation experiments: inverted hierarchy

Decay rate sensitive to
neutrino masses, hierarchy
$m_{\beta\beta} = |\sum U_{ek}^2 m_k|$

$$\left(T_{1/2}^{0\nu\beta\beta}\right)^{-1} = G_{0\nu}\, g_A^4 \left|M^{0\nu\beta\beta}\right|^2 m_{\beta\beta}^2$$

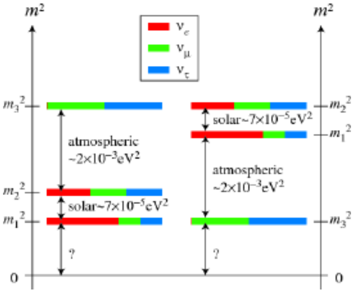

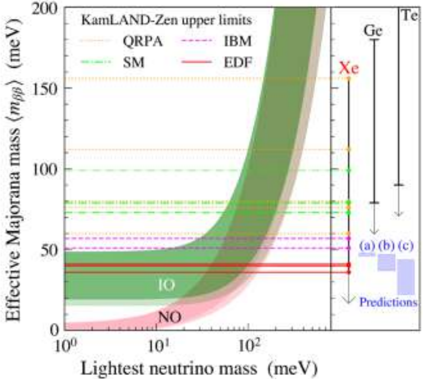

Matrix elements assess
if next-generation experiments
fully cover "inverted hierarchy"

KamLAND-Zen, PRL130 051801(2023)

$0\nu\beta\beta$ decay nuclear matrix elements

Large difference in nuclear matrix element calculations

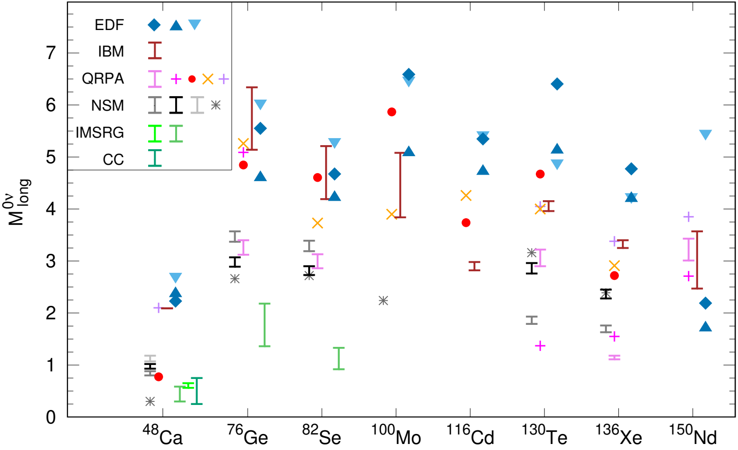

Agostini, Benato, Detwiler, JM, Vissani, Rev. Mod. Phys. 95, 025002 (2023)

Deformation and $0\nu\beta\beta$ NMEs

$0\nu\beta\beta$ decay is disfavoured by quadrupole correlations

$0\nu\beta\beta$ decay very suppressed when nuclei have different structure

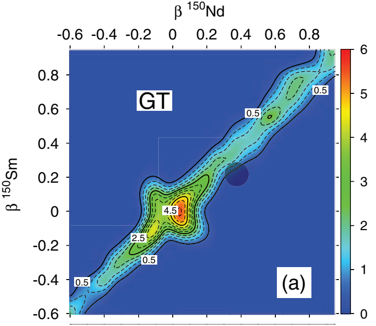

Rodríguez, Martínez-Pinedo
PRL105 252503 (2010)

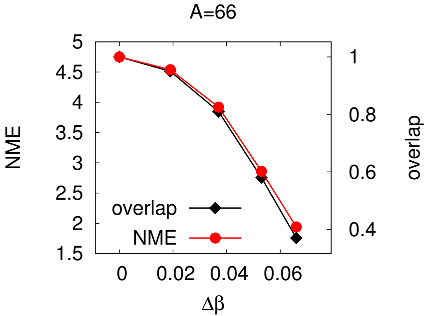

JM, Caurier, Nowacki, Poves
JPCS267 012058 (2011)

Suppression also observed with QRPA Fang et al. PRC83 034320 (2011)

$2\nu\beta\beta$ decay, 2νECEC of ^{124}Xe

Two-neutrino $\beta\beta$ predicted for ^{48}Ca before measurement

Caurier, Poves, Zuker, PLB 252 13(1990)

Recent predictions for 2νECEC ^{124}Xe half-life:

shell model error bar largely dominated by "quenching" uncertainty

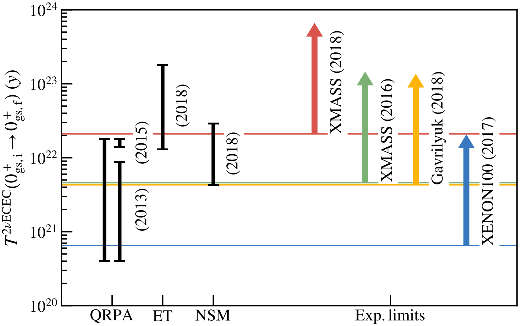

Suhonen
JPG 40 075102 (2013)

Pirinen, Suhonen
PRC 91, 054309 (2015)

Coello Pérez, JM, Schwenk

PLB 797 134885 (2019)

Shell model, QRPA and Effective theory (ET) predictions suggest experimental detection close to XMASS 2018 limit

$2\nu\beta\beta$ decay, 2νECEC of ^{124}Xe

Two-neutrino $\beta\beta$ predicted for ^{48}Ca before measurement
Caurier, Poves, Zuker, PLB 252 13(1990)
Recent predictions for 2νECEC ^{124}Xe half-life:
shell model error bar largely dominated by “quenching” uncertainty

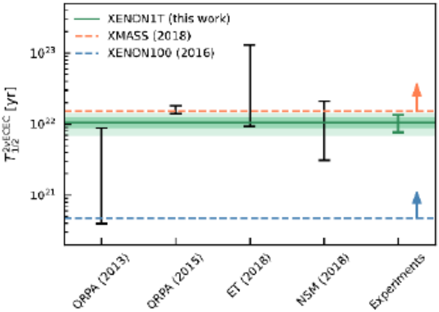

Suhonen
JPG 40 075102 (2013)

Pirinen, Suhonen
PRC 91, 054309 (2015)

Coello Pérez, JM, Schwenk
PLB 797 134885 (2019)

XENON1T
Nature 568 532 (2019)
PRC106, 024328 (2022)

Shell model, QRPA, Effective theory (ET)
good agreement with XENON1T measurement!

$2\nu\beta\beta$ decay to excited states

Two-neutrino $\beta\beta$ predictions to excited states

Benavente, Castillo, Frycz, JM, in preparation

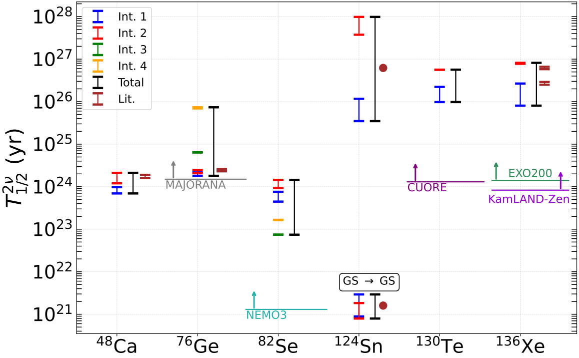

In general, uncertainty due to nuclear Hamiltonian:
Relation to deformation of initial and final states?

^{76}Ge and ^{76}Se: shape invariants

Shape invariants show that difference in deformation varies quite significantly with the shell-model Hamiltonians used

Benavente, Castillo, Frycz, JM, in preparation

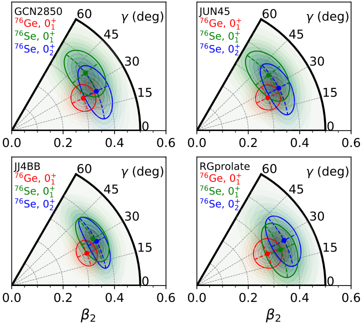

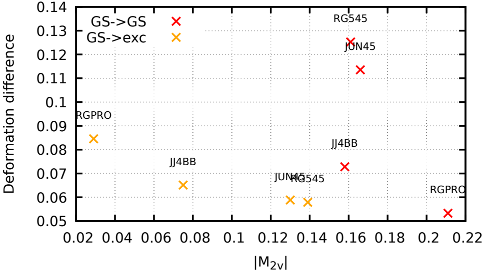

Difference in deformation can explain big part of the value of the two-neutrino $\beta\beta$ decay nuclear matrix elements

$\Longrightarrow$ predict whether $2\nu\beta\beta$ decay in ^{76}Ge measured soon or not!

Outline

Summary

Nuclear deformation within shell model:
energies, B(E2)'s, moments...
shape invariants
variational approach based on mean field

Very consistent shape coexistence picture:
^{40}Ca: spherical, deformed, superdeformed
^{28}Si: oblate, prolate, superdeformed

Application to $\beta\beta$ decay:
close relation between nuclear deformation and nuclear matrix elements
select best shell-model Hamiltonians

Extend calculations to other nuclei and regions across the nuclear chart

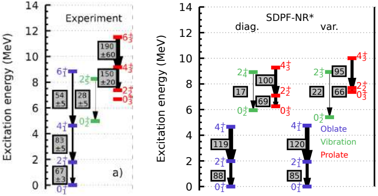

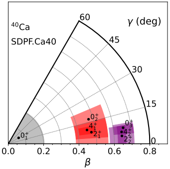

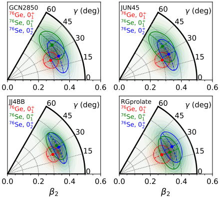

Thank you very much for your attention!

Feel free to ask any questions!

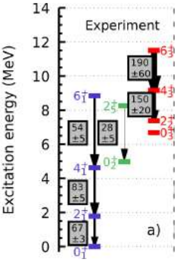

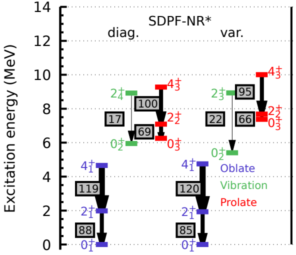

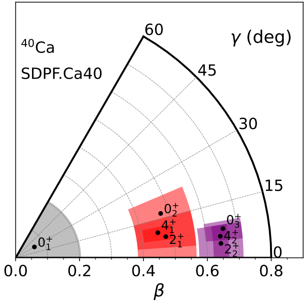

^{28}Si: USDB-MOD vs experiment

Calculations using USDB-MOD interaction describe reasonably well both oblate and prolate bands simultaneously!

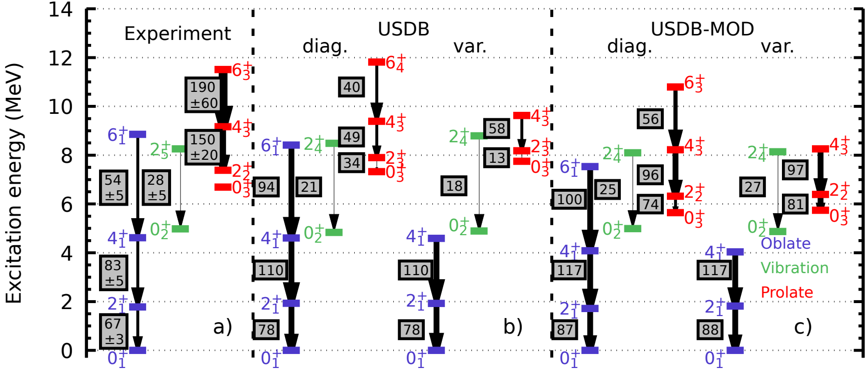

Frycz et al. PRC 110 054326 (2024)

Collective WFs. (USDB-MOD): prolate band

Collective wavefunctions obtained with USDB-MOD
confirm well-defined structure for experimental prolate band

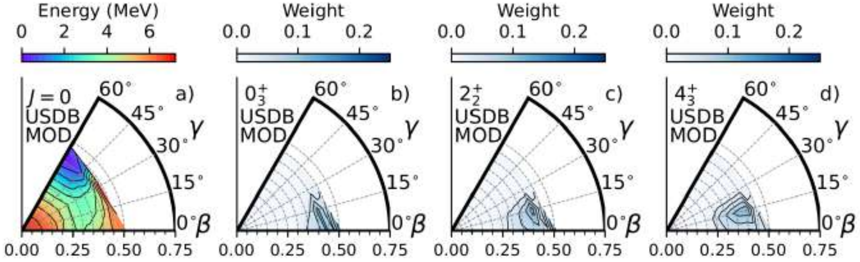

Frycz et al. PRC 110 054326 (2024)

Occupancies of prolate 0^+, 2^+, 4^+ consistent with quasi-SU(3) picture (enhanced $0d_{3/2}$ occupancy)

2^+ quadrupole moment and $0^+ \to 2^+$ quadrupole sum rule consistent with well-deformed prolate band

Shape invariants: USDB-MOD

Different shapes in ^{28}Si well defined, also with new interaction

We can confirm the well-defined character of the oblate and prolate structures by calculation Kumar's shape invariants:

Nucleus	State	β_{RME}	δ_{RME}	β_{SR}	δ_{SR}
Si28 (USDB)	0_1^+	0.45±0.09	52 (41-60)	0.47±0.08	50 (37-60)
	0_2^+	0.39±0.13	52 (44-60)	0.42±0.12	51 (34-60)
	0_3^+	0.47±0.07	11 (0-19)	0.51±0.08	17 (0-32)
Si28 (USDB-MOD)	0_1^+	0.48±0.08	50 (39-60)	0.49±0.08	49 (37-60)
	0_2^+	0.42±0.12	42 (28-60)	0.45±0.13	41 (29-60)
	0_3^+	0.51±0.08	8 (0-18)	0.53±0.08	11 (0-23)